Journal of Applied Mechanics and Technical Physics, Vol. 48, No. 1, pp. 55–64, 2007

TWO REGIMES OF LIQUID FILM FLOW ON A ROTATING CYLINDER

E. A. Karabut

UDC 532.516

A steady flow of a thin film of a viscous incompressible liquid on a rotating cylinder (the cylinder axis is perpendicular to the direction of the force of gravity) is considered. Capillary effects are taken into account on the free surface. Thin-layer equations derived by Pukhnachov, which depend on the Galileo number and capillary number, are solved. If the first parameter equals zero, the force of gravity also equals zero. If the second parameter equals zero, the surface-tension coefficient also equals zero. The values of these parameters that ensure the solution existence and the number of solutions are determined by the method of collocations. One more solution corresponding to the drop-shaped free surface is found numerically. Variations of flow parameters caused by variations of the Galileo number and capillary number are considered. Branching of the solutions is examined numerically.

Key words: *Navier–Stokes equations, free boundary, capillarity, long waves.*

Formulation of the Problem. A solid cylinder of radius a rotates anticlockwise with an angular velocity ω. The cylinder is covered by a liquid film (with viscosity ν, density ρ, and surface-tension coefficient σ). The force of gravity is defined by the acceleration of gravity g. We seek for a steady-state solution: we have to find the film thickness $h(\theta)$, which depends only on the polar angle θ (Fig. 1).

In [1–7], this problem was solved by using various approximations. In the exact unsteady formulation [2], where the film thickness is not assumed to be small, this problem is defined by three dimensionless parameters: Reynolds number $\mathrm{Re} = a^2\omega/\nu$, Galileo number $\mathrm{G} = ga/(\omega\nu)$, and capillary number $C = \sigma/(\rho a\omega\nu)$.

Introduction of a small parameter ε by

$$h = \varepsilon a H$$

allows considering films of small thickness. For $\varepsilon \to 0$, the function H and its derivatives with respect to ε are assumed to be finite. In addition, the existence of the following limits is postulated for $\varepsilon \to 0$:

$$C\varepsilon^3 \to 3\alpha, \qquad \mathrm{G}\,\varepsilon^2 \to 3\gamma, \qquad \mathrm{Re}\,\varepsilon^2 \to 0.$$

Under these conditions, the unknown function $H(\theta, t)$, which describes unsteady deformation of the film, is found from the equation

$$H_t + \alpha[H^3(H_{\theta\theta\theta} + H_\theta)]_\theta + (H - \gamma H^3 \cos\theta)_\theta = 0 \tag{1}$$

and depends on the dimensionless parameters α and γ. The behavior of this equation was studied in [6].

In the steady case, Eq. (1) is integrated one time, and the unknown function $H(\theta)$ is determined by the ordinary differential equation

$$\alpha H^3(H''' + H') = \gamma H^3 \cos\theta - H + Q,$$

where Q is the dimensionless liquid flow through the film cross section.

Lavrent'ev Institute of Hydrodynamics, Siberian Division, Russian Academy of Sciences, Novosibirsk 630090; karabut@hydro.nsc.ru. Translated from Prikladnaya Mekhanika i Tekhnicheskaya Fizika, Vol. 48, No. 1, pp. 68–78, January–February, 2007. Original article submitted January 13, 2006; revision submitted March 27, 2006.

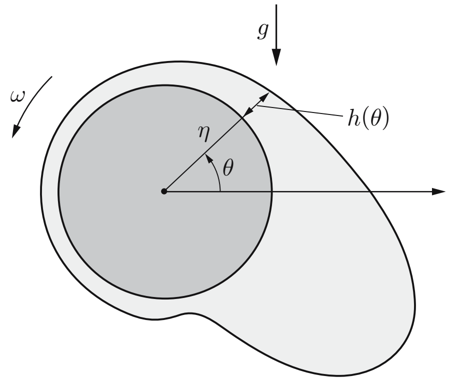

Fig. 1. Sketch of the flow.

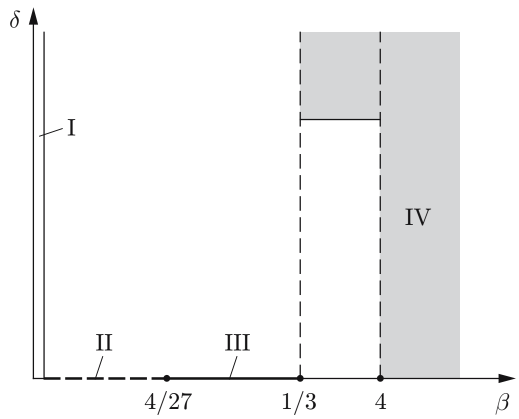

Fig. 2

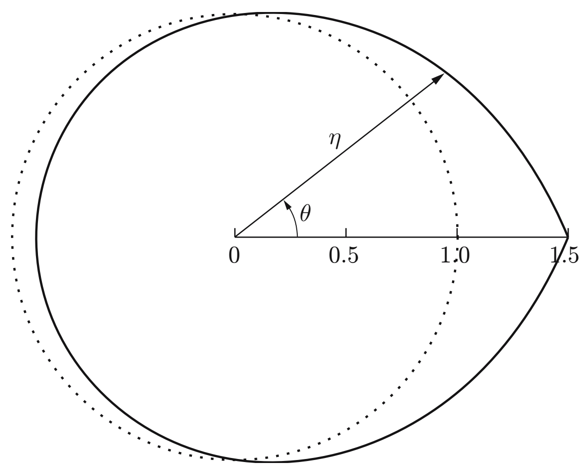

Fig. 3

Fig. 2. Domains of existence of solutions of problem (2), (3) in the plane (β, δ) (data of [1–3, 6]): power series (I), unique solution (II), no solutions (III and IV).

Fig. 3. Dependence $\eta(\theta)$ in the absence of capillarity ($\delta = 0$): the dotted and solid curves refer to $\beta = 0$ and 4/27, respectively.

Introducing the notation

$$\eta = Q^{-1}H, \qquad \delta = \alpha Q^3, \qquad \beta = \gamma Q^2,$$

we can determine the film thickness $\eta(\theta)$ by solving the problem

$$\delta(\eta''' + \eta') = \beta \cos\theta - 1/\eta^2 + 1/\eta^3; \tag{2}$$

$$\eta(\theta + 2\pi) = \eta(\theta). \tag{3}$$

Problem (2), (3) depends on the parameters δ and β. The question on the number of solutions of problem (2), (3) can be partly answered by the theorem proved in [2].

Theorem 1. *There exist parameters δ and β, such that problem* (2), (3) *has at least two solutions.*

The number of solutions, their type and character can be found only numerically. The goal of the present work was to determine a set of points in the parametric plane (δ, β) for which the problem considered has solutions and the number of solutions by numerical methods, as well as to study the solutions.

We have to find where approximately in the parametric plane (δ, β) we have to seek for a region where the solution of problem (2), (3) exists. Figure 2 shows the data of [1–3, 6].

The following is known.

1. The domain of solution existence is located in the first quadrant of the parametric plane (δ, β), because $\delta \geqslant 0$ and $\beta \geqslant 0$.

2. No solutions exist for $\beta > 4$.

3. If the value of δ is sufficiently high and $\beta > 1/3$, no solutions exist.

4. For $\delta = 0$ and $\beta \in [0; 4/27]$, there exists a unique solution. For $\delta = 0$ and $\beta \in (4/27; \infty)$, no solutions exist.

5. For $\beta = 0$, there exists a solution $\eta = 1$. For small β, there always exists a solution representable in the form of a series in powers of β:

$$\eta = 1 + \beta\cos\theta + \beta^2\Big(\frac{3}{2} + \frac{3}{2}\,\frac{1}{1+36\delta^2}\,\cos 2\theta - \frac{9\delta}{1+36\delta^2}\,\sin 2\theta\Big) + O(\beta^2). \tag{4}$$

The absence of capillarity ($\delta = 0$) considered in [3] is the simplest case, because the differential equation (2) becomes algebraic. For $\delta = 0$ and $\beta = 4/27$, a spinode appears on the free surface. The dependence $\eta(\theta)$ for this case is shown in Fig. 3 in a polar coordinate system. (Figures 3 and 7–9 do not show the internal solid cylinder, which is actually shrunk into a point. It is impossible to show this cylinder, because its radius is equal to infinity in the thin-film approximation.) The dotted curve shows the unit circumference, which is the plot of the function $\eta(\theta)$ for $\delta = 0$ and $\beta = 0$.

Analytical Continuation of the Solution. Problem (2), (3) is approximated by two methods by a system of algebraic equations of rather large dimension and is solved numerically by the Newton method. The convergence of the Newton method is known to depend to a large extent on the initial approximation. If the initial approximation is chosen successfully, iterations converge and yield this or that branch of the solution of the approximated problem. Otherwise, the iterative process diverges.

The solution was analytically continued in the parametric plane (δ, β) as follows. Let a solution of the system of algebraic equations be known for $\delta = \delta_0$ and $\beta = \beta_0$. This solution is chosen as the initial approximation for finding the solution at another point of the parametric plane $\delta = \delta_0 + \Delta\delta$, $\beta = \beta_0 + \Delta\beta$. If the steps $(\Delta\delta, \Delta\beta)$ are sufficiently small and the Jacobian of the system of algebraic equations differs from zero, the Newton method always converges with such an initial approximation. Moving in this manner along an arbitrary path emanating from the point (δ_0, β_0), one can analytically continue the chosen branch of the solution to a given point (δ, β).

At each step, we calculated the Jacobian whose vanishing (in real computations, a change in sign) means that a bifurcation point is found. Either a further analytical continuation of the solution along the chosen path is impossible or it is possible but the initial approximation in the vicinity of the bifurcation point should be chosen in a special manner.

Method of Collocations. Problem (2), (3) is extremely sensitive to minor variations of the parameters δ and β; therefore, a fairly accurate algorithm is needed for solving this problem. High accuracy can be provided by projection algorithms (such as the Galerkin method). As we have to find a periodic solution of the equation

$$\delta\eta^3(\eta''' + \eta') - \beta\eta^3\cos\theta + \eta - 1 = 0, \tag{5}$$

we can naturally use trigonometric polynomials as the basic functions. We seek for the solution in the form

$$\eta = a_0 + \sum_{n=1}^{N}(a_n\cos n\theta + b_n\sin n\theta). \tag{6}$$

The number N determines the number of harmonics used; higher values of N ensure better accuracy of computations. The quantities to be determined are the coefficients of the trigonometric polynomial

$$a_0, a_1, \ldots, a_N, b_1, b_2, \ldots, b_N. \tag{7}$$

Generally speaking, solution (6) does not satisfy Eq. (5). Among the projection methods, the simplest one for implementation is the method of collocations, in which the equation has to be satisfied in a finite number of points. We substitute solution (6) into Eq. (5) and require that the left side of the equation equals zero at $2N+1$ points $\theta_j = 2\pi j/(2N+1)$. As a result, we obtain a system of $2N+1$ equations

$$f_j(a_0, a_1, \ldots, a_n, b_1, b_2, \ldots, b_n; \delta, \beta) = 0 \qquad (j = \overline{0, 2N}\,) \tag{8}$$

TABLE 1

Method of collocations		Finite-difference method	
N	$\eta(0)$	M	$\eta(0)$
5	**1.537**53933335633	20	**1.5**6546924158431
10	**1.537386**89936422	80	**1.53**903374468117
15	**1.53738674**169974	320	**1.537**48926620556
20	**1.53738674261**031	1280	**1.5373**9314873436
25	**1.5373867426113**7	2560	**1.53738**834412210

for finding $2N+1$ unknowns (7). The formulas for Eqs. (8) and the Jacobian $\partial f_j/\partial a_n$, $\partial f_j/\partial b_n$ can be readily obtained.

Finite-Difference Method. In the present work, the finite-difference method plays an auxiliary role: it is used to monitor the accuracy of the method of collocations. We divided the interval $\theta \in [0; 2\pi]$ into M segments of identical length $\Delta\theta = 2\pi/M$. In grid nodes $\theta_j = \Delta\theta(j-1)$, we consider the film thickness $\eta_j = \eta(\theta_j)$. The unknowns to be determined are

$$\eta_1, \eta_2, \ldots, \eta_M. \tag{9}$$

Replacing the first and third derivatives by the finite differences

$$\eta_j' = \frac{\eta_{j+1} - \eta_{j-1}}{2\Delta\theta}, \qquad \eta_j''' = \frac{\eta_{j+2} - 2\eta_{j+1} + 2\eta_{j-1} - \eta_{j-2}}{2(\Delta\theta)^3}$$

and substituting them into Eq. (5), we obtain its finite-difference approximation

$$f_j = \eta_j^3[S_1(\eta_{j+2} - \eta_{j-2}) + S_2(\eta_{j+1} - \eta_{j-1})] - \beta\eta_j^3 \cos\theta_j + \eta_j - 1 = 0, \tag{10}$$

where S_1 and S_2 are constants. Adding the periodicity condition

$$\eta_{M+1} = \eta_1, \quad \eta_{M+2} = \eta_2, \quad \eta_0 = \eta_M, \quad \eta_{-1} = \eta_{M-1}, \tag{11}$$

we obtain a system of M equations from Eqs. (10) and (11)

$$g_j(\eta_1, \eta_2, \ldots, \eta_M; \delta, \beta) = 0 \qquad (j = \overline{1, M}\,) \tag{12}$$

to find M unknowns (9). System (12) is also solved by the Newton method.

First Solution. The first solution is the solution of problem (2), (3) coinciding with solution (4) for small β. Note, in the absence of capillarity ($\delta = 0$) for $\beta \in [0; 4/27]$, this is the only possible solution. To find the first solution for values of β that are not small, we analytically continue the power series (4) as the initial approximation in the Newton method from the region of small β. For this purpose, both the method of collocations and the finite-difference method are used.

Table 1 shows the values of $\eta(0)$, i.e., the film thickness for $\theta = 0$ for the first solution ($\beta = 0.2$ and $\delta = 0.1$) calculated by the method of collocations and by the finite-difference method. The valid signs after the decimal point are marked bold. It follows from Table 1 that the method of collocations is more efficient and less expensive than the finite-difference method, which yields the same results but requires much more effort. In our work, we mainly used the method of collocations with $N = 20$ (this number of harmonics allows rather fast computations with approximately 10 digits after the decimal point); the finite-difference method was used in certain cases to verify the accuracy.

The shape of the free surface for the first solution is weakly deformed and is close to a circumference. The greatest deformation of the free surface is reached for $\delta = 0$ and $\beta = 4/27$ (see Fig. 3).

In the analytical continuation of the solution from the region of small β along the straight line $\delta = \text{const}$, an increase in β ensures reaching a limiting value $\tilde{\beta}(\delta)$ with which the Jacobian of the system vanishes. It will be shown below than the bifurcation points found are turning points: further analytical continuation into the region $\beta > \tilde{\beta}(\delta)$ is impossible. Thus, a closed domain with the first solution existing at each point of this domain is found in the parametric plane (δ, β) (Fig. 4). This domain is a curved half-band bounded on the right by the curve $\beta = \tilde{\beta}(\delta)$; as $\delta \to \infty$, the curved band becomes straight: $0 \leqslant \beta \leqslant \beta^*$.

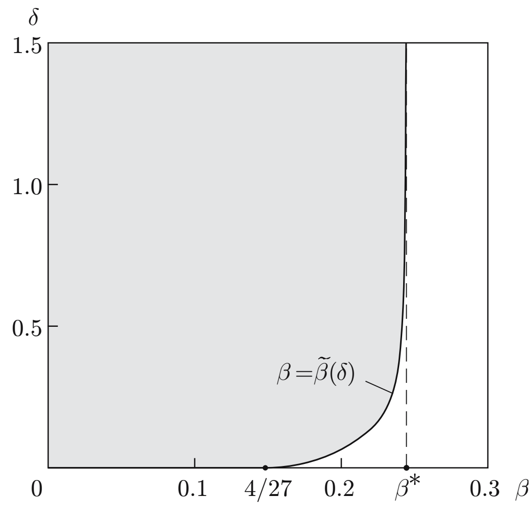

Fig. 4. Domain of existence of solutions.

Second Solution. According to Pukhnachov's theorem, there has to exist one more solution, which will be called the second solution. To find this solution by the Newton method, we have to find the initial approximation and perform an analytical continuation by straight lines $\beta = \text{const}$ from infinitely remote points $\delta = \infty$ in the direction of decreasing δ.

The limit $\delta \to \infty$ corresponds to a strongly capillary liquid, and Eq. (2) becomes linear:

$$\eta''' + \eta' = 0.$$

This equation has three linearly independent solutions:

$$1; \quad \cos\theta; \quad \sin\theta. \tag{13}$$

Hence, the general solution has the form

$$\eta = s + q\cos\theta - \tau\sin\theta. \tag{14}$$

The constants s, q, and τ, however, cannot be arbitrary, because the solution of the original problem (2), (3) has to satisfy three integrals. These integrals can be obtained by multiplying Eq. (2), respectively, by three solutions (13) and then integrating from 0 to 2π:

$$\int\limits_0^{2\pi} \frac{\eta - 1}{\eta^3}\, d\theta = 0; \tag{15}$$

$$\int\limits_0^{2\pi} \frac{\eta - 1}{\eta^3} \cos\theta\, d\theta = \pi\beta; \tag{16}$$

$$\int\limits_0^{2\pi} \frac{\eta - 1}{\eta^3} \sin\theta\, d\theta = 0. \tag{17}$$

Relations (15)–(17) have to be satisfied for all values of the parameter δ, including $\delta = \infty$. Substituting Eq. (14) into (15)–(17) and integrating these expressions (the integrals are taken with the use of the theory of residues), we obtain relations between the parameters s, q, and τ. From Eqs. (15), (16), and (17), respectively, we obtain

$$\frac{\pi[s(2q^2 - 2s^2 + 2\tau^2 + 3s) + (q^2 + \tau^2 - s^2)]}{(s^2 - q^2 - \tau^2)^{5/2}} = 0; \tag{18}$$

$$\frac{\pi q(2q^2 - 2s^2 + 2\tau^2 + 3s)}{(s^2 - q^2 - \tau^2)^{5/2}} = \pi\beta; \tag{19}$$

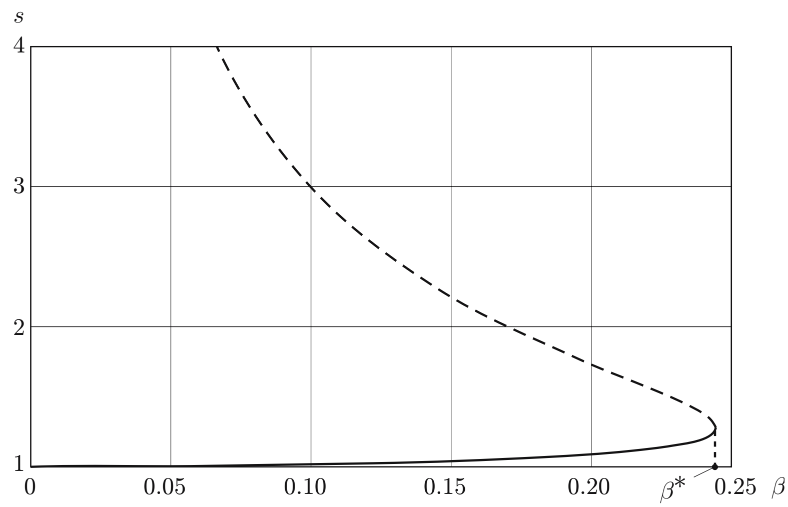

Fig. 5. Dimensionless film thickness s averaged over the circumference versus the force of gravity β ($\delta = \infty$): the solid and dashed curves show the first and second solutions, respectively.

$$\frac{\pi\tau(2q^2 - 2s^2 + 2\tau^2 + 3s)}{(s^2 - q^2 - \tau^2)^{5/2}} = 0. \tag{20}$$

It follows from Eq. (19) that the expression in brackets $2q^2 - 2s^2 + 2\tau^2 + 3s$ cannot be equal to zero; hence, we obtain $\tau = 0$ from Eq. (20). With allowance for this condition, Eqs. (18), (19) are transformed to

$$(2s + 1)q^2 - 2s^2(s - 1) = 0; \tag{21}$$

$$\frac{q(2q^2 - 2s^2 + 3s)}{(s^2 - q^2)^{5/2}} = \beta. \tag{22}$$

We can find q from Eq. (21); taking into account the estimates made in [2]

$$0 \leqslant \beta q \leqslant 2, \qquad s \geqslant 1, \tag{23}$$

we use the plus sign in extracting the root:

$$q = s\sqrt{2(s - 1)/(2s + 1)}.$$

Substituting the resultant expression into Eq. (22), we find

$$\beta = \frac{2s + 1}{s^3}\sqrt{\frac{2}{27}\,(s - 1)}. \tag{24}$$

Thus, s is determined from the equation

$$27\beta^2 s^6 - 8s^3 + 6s + 2 = 0. \tag{25}$$

Equation (25) has two real roots whose dependence on β obtained numerically is plotted in Fig. 5.

Note that the quantity s is either the mean thickness of the film or the film thickness for $\theta = \pm\pi/2$. Figure 5 shows the dependence $s(\beta)$ for $\delta = \infty$. For each value of β in the interval $(0, \beta^*)$, there are two values of these thicknesses. Hence, problem (2), (3) has two solutions. The solid curve in Fig. 5 refers to the first solution (as $\beta \to 0$, all thicknesses tend to unity). There also exists the second solution shown by the dashed curve (as $\beta \to 0$, it increases unlimitedly). For $\beta \to \beta^* = \tilde{\beta}(\infty)$, the solutions coincide, and there are no solutions for $\beta > \beta^*$. The value of β^* is easily found. Indeed, for $\beta = \beta^*$, Eq. (25) has a double root s^*; hence, the derivative of Eq. (25) with respect to s should have the same root:

$$27 \cdot 6\beta^2 s^5 - 24s^2 + 6 = 0. \tag{26}$$

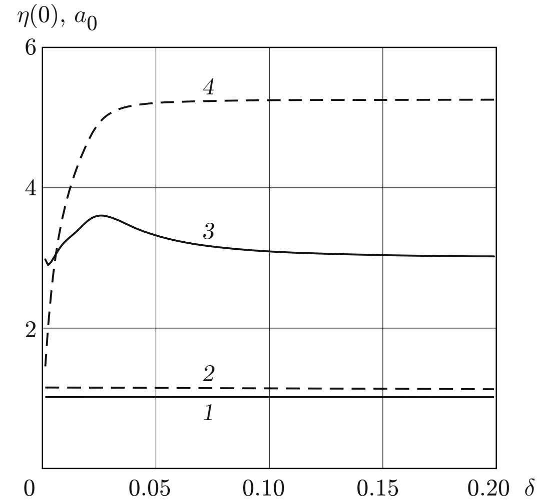

Fig. 6. Film thickness $\eta(0)$ for $\theta = 0$ (dashed curves) and mean thickness a_0 (solid curves) versus the surface-tension coefficient δ ($\beta = 0.1$): curves 1 and 2 show the first solution; curves 3 and 4 refer to the second solution.

If Eq. (26) is subtracted from Eq. (25) multiplied by 6, one of the roots of the resultant equation

$$4s^3 - 5s - 2 = 0 \tag{27}$$

should also be s^*. The cubic equation (27) has three real roots:

$$-\frac{1}{2}, \quad \frac{1-\sqrt{17}}{4}, \quad \frac{1+\sqrt{17}}{4}.$$

The first two roots are negative; by virtue of estimate (23), they do not fit. Therefore,

$$s^* = (1+\sqrt{17}\,)/4 \simeq 1.28078.$$

Substituting this value into Eq. (24), we obtain

$$\beta^* = (1/24)\sqrt{17\sqrt{17} - 107/3} \simeq 0.24447.$$

Thus, for $\delta = \infty$, the second solution is presented by explicit formulas. Using these formulas as the initial approximation and analytically continue the straight lines $\beta = \text{const}$, we can find the second solution for finite values of δ. For finite fixed values of δ, the dependence of the film thickness on the parameter β remains qualitatively unchanged and similar to the dependence plotted in Fig. 5. As previously, there are two solutions for $\beta \in (0; \tilde{\beta}(\delta))$, which coincide for $\beta = \tilde{\beta}(\delta)$, and no solutions exist for $\beta > \tilde{\beta}(\delta)$.

Thus, the second solution coincides with the first one on the right boundary of the curved half-band shown in Fig. 4. On the left boundary, the second solution unlimitedly increases as $\beta \to 0$ and does not exist for $\beta = 0$, whereas the first solution remains finite. The curved band has also a third (lower) boundary: $\delta = 0$. It seems of interest to study the behavior of the second solution as $\delta \to 0$, because, as was mentioned above, problem (2), (3) has a unique solution in the absence of capillarity ($\delta = 0$). It was originally assumed that two variants of the behavior of the second solution are possible: either it coincides with the first solution (as on the right boundary) or increases unlimitedly (as on the left boundary). The situation on the lower boundary, however, is more complicated: as $\delta \to 0$, both variants are observed simultaneously: two solutions coincide and the second solution increases unlimitedly (Fig. 6). The first type of the behavior is illustrated by the dashed curves in Fig. 6. For a fixed value of β and $\delta \to 0$, the film thicknesses calculated for the first and second solutions for $\theta = 0$ are almost identical. Both thicknesses tend to the known limit corresponding to a capillary-free film. The other variant of the behavior is shown by the solid curves in Fig. 6. It is seen that the mean film thickness [or the coefficient a_0 in the trigonometric polynomial (6)], which tends to the known capillary-free limit for the first solution, obviously does not tend to this limit for the second solution, and it is not clear whether it tends to any limit at all in the latter

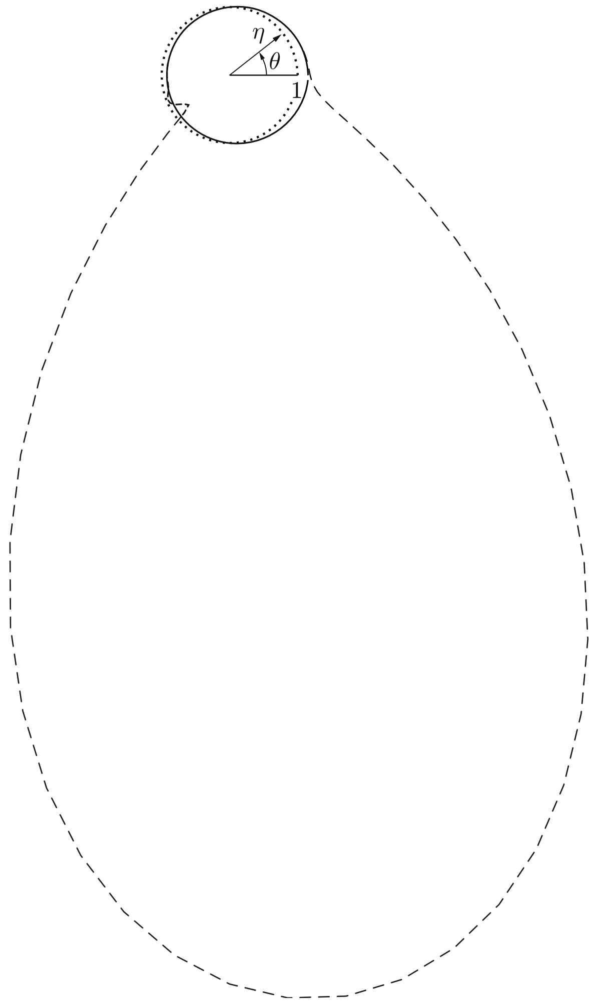

Fig. 7. Dependence $\eta(\theta)$ for $\beta = 0.1$ and $\delta = 0.0005$: the solid and dashed curves show the first and second solutions, respectively; the dotted curve is the unit circumference.

case. These qualitatively different variants of the film-thickness behavior at a point and the mean film thickness for the second solution is explained in Fig. 7. In a polar coordinate system, Fig. 7 shows the film thickness for the first and second solutions for $\beta = 0.1$ and a very small value of δ. Approximately on one half of the free surface, the first solution coincides with the second one, whereas they are significantly different on the other half of the free surface.

Despite the thin-film approximation used, the second solution is physically meaningful: it describes the regime with a hanging drop. With decreasing δ, i.e., with decreasing surface tension, the size of the hanging portion of the drop becomes substantially greater. Note that the increase in film thickness does not contradict the thin-film theory, because the film thickness is still small, as compared with the infinitely large radius of the cylinder.

For a fixed value of β, Fig. 8 shows the dynamics of the free surface shape. The parameter δ decreases with a constant step from 0.01 to 0.001. With such a small variation of δ, the shape of the free surface in the first solution is almost unchanged and is almost a regular circle. In the second solution, the shape of the free surface changes significantly. As the capillarity decreases (with decreasing δ), the second solution predicts that a hanging drop is formed on the free surface and starts increasing.

It is not completely clear what happens to the second solution with a further decrease in δ. Apparently, the second solution cannot be continued to $\delta = 0$ because of secondary bifurcations, which occur at very small values $\delta = 10^{-5}$–10^{-8}. A change in the sign of the Jacobian was registered, and spinodes were found on the free surface.

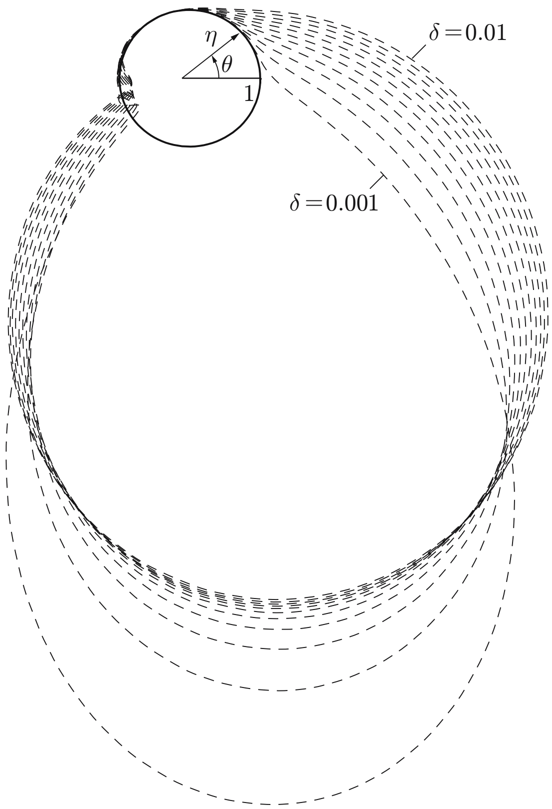

Fig. 8

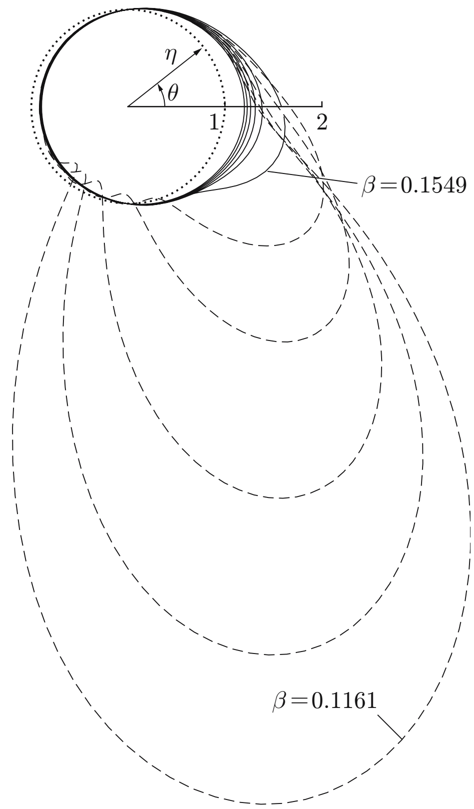

Fig. 9

Fig. 8. Dependence $\eta(\theta)$ for $0.001 \leqslant \delta \leqslant 0.010$ ($\beta = 0.1$): the solid and dashed curves refer to the first and second solutions, respectively.

Fig. 9. Dependence $\eta(\theta)$ for $0.1161 \leqslant \beta \leqslant 0.1549$ ($\delta = 0.001$): the solid and dashed curves show the first and second solutions, respectively; the dotted curve is the unit circumference.

In this case, an additional study is needed. It is difficult to construct a reliable numerical algorithm because the secondary bifurcations occur at very low values of δ.

Figure 9 also shows the shapes of the free surface ($\delta = 0.001$, the parameter β changes with a constant step from 0.1161 to 0.1549). For the maximum possible value $\beta = 0.1549$, the first and second solutions coincide, and there are no solutions for $\beta > 0.1549$. For the first solution, the overall film thickness decreases with decreasing β and tends to a unit circumference as $\beta \to 0$, which is shown by the dotted curve in Fig. 9. For the second solution, the film thickness increases with decreasing β, and the free surface acquires a drop-shaped form.

Conclusions. It is shown that the range of existence of the solution of problem (2), (3), which describes a thin capillary film on the surface of a rotating cylinder, is a curved band (see Fig. 4) with three boundaries: right, left, and lower ones. There exists the known classical solution at each point of this half-band. At all points of the half-band, except for a small neighborhood of the lower boundary, there also exists the second solution. The solutions coincide on the right boundary. When approaching the left boundary, the film thickness tends to unity for the first solution and unlimitedly increases for the second solution. The second solution is physically meaningful: it describes the flow with a hanging drop; apparently, this solution is unstable, which also reflects the physical nature of the phenomenon, because hanging drops may tear off from the film.

The author is grateful to V. V. Pukhnachov for assistance in this work and useful discussions.

This work was supported by the Russian Foundation for Basic Research (Grant No. 04-01-00355) and Foundation "Leading Scientific Schools of Russia" (Grant No. NSh-5873.2006.1).

REFERENCES

1. V. V. Pukhnachev, “Motion of a liquid film on the surface of a rotating cylinder,” *J. Appl. Mech. Tech. Phys.*, **18**, No. 3, 344–350 (1977).
2. V. V. Pukhnachov, “Capillary/gravity film flow on the surface of a rotating cylinder,” *J. Math. Sci.*, **130**, No. 4, 4871–4883 (2005).
3. H. K. Moffatt, “Behaviour of viscous film on the outer surface of a rotating cylinder,” *J. Mech.*, **187**, 651–673 (1977).
4. E. B. Hansen and M. A. Kelmanson, “Steady, viscous, free-surface flow on a rotating cylinder,” *J. Fluid Mech.*, **272**, 91–107 (1994).
5. R. G. Petersen, P. K. Jimack, and M. A. Kelmanson, “On the stability of viscous free-surface flow supported by a rotating cylinder,” *Proc. Roy. Soc. London, Ser. A*, **457**, 1427–1445 (2001).
6. E. J. Hinch and M. A. Kelmanson, “On the decay and drift of free-surface perturbations in viscous thin-film flow exterior to a rotating cylinder,” *Proc. Roy. Soc. London, Ser. A*, **459**, 1193–1213 (2003).
7. E. J. Hinch, M. A. Kelmanson, and P. D. Metcalfe, “Shock-like free-surface perturbations in low-surface-tension, viscous, thin-film flow,” *Proc. Roy. Soc. London, Ser. A*, **460**, 2975–2991 (2004).